

Elimination of Multiple Access Interference in Ultrashort Pulse OCDMA Through Nonlinear Polarization Rotation

Changjian Guo, Xuezhi Hong, and Sailing He, *Senior Member, IEEE*

Abstract—A multiple access interference elimination scheme based on nonlinear polarization rotation (NPR) is proposed for ultrashort pulse optical code-division multiple access (OCDMA). This scheme is experimentally investigated in a four-user and 2.5-Gb/s coherent OCDMA system encoded/decoded by 127-chip superstructured fiber Bragg gratings. The measured bit-error-rate results of the NPR-based thresholder are also compared with those of a conventional supercontinuum-based thresholder in both the back-to-back and 20-km transmission cases. Our proposed scheme has the advantage of colorless operation over *C*-band.

Index Terms—Fiber-optical communication, multiple-access interference (MAI), optical code-division multiple access (OCDMA), superstructured fiber Bragg grating (SSFBG).

I. INTRODUCTION

OPTICAL code-division multiple access (OCDMA) [1] has been attracting much research interest during the past decades. In an OCDMA system, each user is assigned a unique signature (called an optical code), and the encoded data streams of all users can be then transmitted through the same medium. OCDMA techniques can offer various advantages, including the possibility of full asynchronous operation, flexible network management, the potential of security enhancement for the physical layer, etc.

Multiple access interference (MAI) is considered as one of the main sources that limit the bit-error-rate (BER) performance and maximal number of simultaneous users in an OCDMA system [2], [6]. Besides the progress in various coding techniques, efforts have been made on hardware techniques to eliminate or reduce the MAI. One choice is the optical time gating [2], [3], which shows good performance. However, its requirement for optical clock recovery and timing coordination makes the receiver more complicated and less cost-effective. An alternative choice is the optical thresholder, which allows asynchronous operation. Various technologies, including second-harmonic generation (SHG) in periodically poled lithium niobate (PPLN) [4], supercontinuum (SC) generation

Manuscript received March 30, 2009; revised June 03, 2009. First published July 28, 2009; current version published September 25, 2009.

C. Guo is with the State Key Laboratory of Modern Optical Instrumentation, Centre for Optical and Electromagnetic Research, Zhejiang University, Hangzhou 310058, China, and also with Queen's University, Kingston, ON K7L4M3, Canada (e-mail: guocj@coer.zju.edu.cn).

X. Hong and S. He are with the State Key Laboratory of Modern Optical Instrumentation, Centre for Optical and Electromagnetic Research, Zhejiang University, Hangzhou 310058, China (e-mail: hongxuezhi@coer.zju.edu.cn; sailing@zju.edu.cn).

Color versions of one or more of the figures in this letter are available online at <http://ieeexplore.ieee.org>.

Digital Object Identifier 10.1109/LPT.2009.2028158

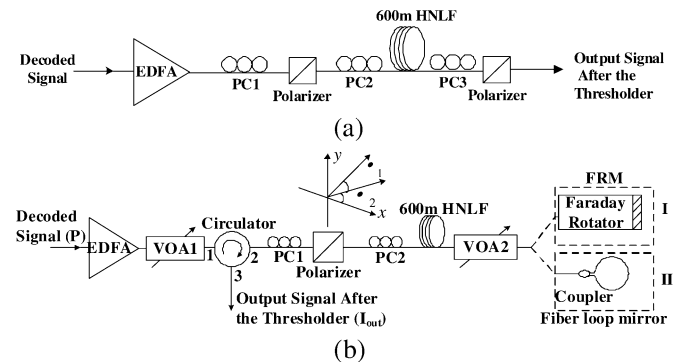


Fig. 1. Structure of the proposed optical thresholder based on the NPR effect. (a) Transmission mode. (b) Case I corresponds to a reflective mode using an FRM and case II corresponds to a reflective mode using a fiber loop mirror. (EDFA: erbium doped fiber amplifier; VOA: variable optical attenuator).

in a highly nonlinear fiber (HNLf), and a dispersion-flattened fiber (DFF) [5], have been used for optical thresholding. Optical thresholders based on SHG and SC are used extensively [6], [7] since they are easy to implement. However, all these thresholders are wavelength dependent, and typically require custom-made bandpass filters.

Intensity-dependent polarization rotation occurs when strong optical fields pass through a nonlinear medium [8]. Various applications of this nonlinear polarization rotation (NPR) effect have been found, including passive mode-locked erbium fiber lasers [9], optical pulse shaping [10], wavelength conversion [11], etc.

In this letter, we propose a novel cost-effective MAI elimination scheme that enables colorless operation. The proposed scheme is based on the NPR effect, and uses commercial low-cost elements including a Faraday rotation mirror (FRM) and an HNLf. We then demonstrate a 127-chip superstructured fiber Bragg grating (SSFBG) coded, four-user, 2.5-Gb/s coherent OCDMA system using our proposed scheme as the optical thresholder. Finally, we compare the performance of our NPR-based thresholder with a conventional SC-based thresholder.

II. PROPOSED OPTICAL THRESHOLDER BASED ON NPR

Fig. 1 shows the structures of our proposed optical thresholder based on the NPR effect. An NPR-based thresholder can be implemented in two modes: a transmission mode [Fig. 1(a)] and a reflective mode [Fig. 1(b)]. The two structures depicted in Fig. 1 are similar except that the output from the HNLf is detected after another polarizer [see, Fig. 1(a)] in the transmission mode, while it is looped back by either an FRM [case I in

Fig. 1(b)] or a fiber loop mirror [case II in Fig. 1(b)] in the reflective mode.

The principle of the NPR-based thresholder is as follows. The polarized light undergoes birefringence in the HNLF. When the intensity of the linearly polarized incident light is weak, only linear birefringence is present. The orientation and ellipticity of the output light polarization is fully determined by the length and the linear birefringence of the HNLF. However, when the intensity of the linearly polarized incident light is strong, the extra nonlinear polarization rotation induced by the Kerr effect must be considered. As the extra nonlinear polarization rotation depends on the light intensity, a polarizer can be employed to obtain an intensity-dependent output, thus forming an optical thresholder. By carefully adjusting the PCs, the linear birefringence can be canceled in structures, shown in Fig. 1(a) and (b) case II, and thus, only the nonlinear part is left. However, the linear birefringence in Fig. 1(b) (case I) will be automatically compensated by the FRM: a 90° polarization change induced by the FRM interchanges the fast axis component and slow axis component of the incident light. Thus, the linear birefringence, i.e., the linear phase delay between the two components, will be canceled after backward propagation. Both architectures in Fig. 1 were evaluated in our test bed and gave very similar performance. However, the unique characteristic of automatic compensation of linear birefringence in Fig. 1(b) (case I) makes it much easier to achieve an optimal output. Thus, we will focus on this structure hereafter.

The linear and nonlinear phase delays between the fast- and slow axis components (after the HNLF), which are induced by the linear and nonlinear birefringences, respectively, can be expressed as follows [8]:

$$\begin{cases} \phi_L = (n_y - n_x)\beta L \\ \phi_{NL} = -\frac{1}{3}\beta P L \cos(2\alpha_2). \end{cases} \quad (1)$$

The output power intensity I_{out} can be calculated by

$$I_{out} = \frac{1}{2}(1 - \alpha)^2 P \cos^2 \alpha_1 \sin^2(2\alpha_2) [1 - \cos(\Delta\phi_{NL})] \quad (2)$$

where P is the input power intensity, $\beta = 2\pi/\lambda$ is the propagation constant, n_x and n_y are the linear birefringence coefficients, $L = 600$ (in meters) is the length of HNLF, $\gamma = 10$ (in $\text{watts}^{-1} \cdot \text{kilometer}^{-1}$) is the nonlinear coefficient of the HNLF, α is the attenuation rate of the variable optical attenuator (VOA2), α_1 is the angle between the polarization direction of the input signal and the polarization direction of the polarizer, and α_2 is the angle between the polarization direction of the polarizer and the fast axis of the HNLF. Angles α_1 and α_2 can be adjusted by polarization controllers PC1 and PC2. Fig. 2 shows the transfer function and the measured waveforms before [Fig. 2 (top)] and after [Fig. 2 (bottom)] our optical thresholder based on the NPR effect.

III. EXPERIMENTS AND DISCUSSION

The performance of the proposed optical thresholder is experimentally investigated in our 127-chip SSFBG-coded, four-user, and 2.5-Gb/s coherent OCDMA system, as shown in Fig. 3(a). An optical pulse train of about 1.5 ps was generated by a mode-locked fiber laser. The repetition rate of the pulse train is 9.953 GHz, and the center wavelength was tuned to 1550 nm. This pulse train was converted to 2.488 GHz and

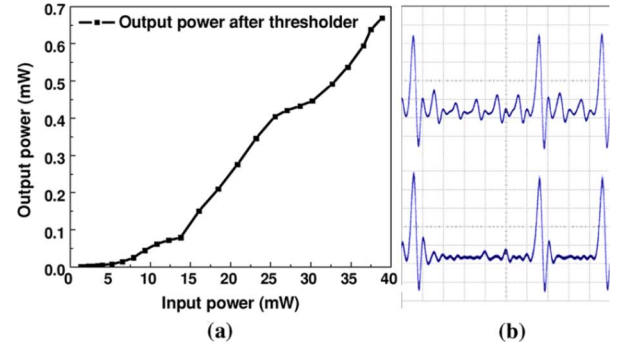


Fig. 2. (a) Power transfer function. (b) Waveforms measured: (top) before and (bottom) after our NPR-based optical thresholder.

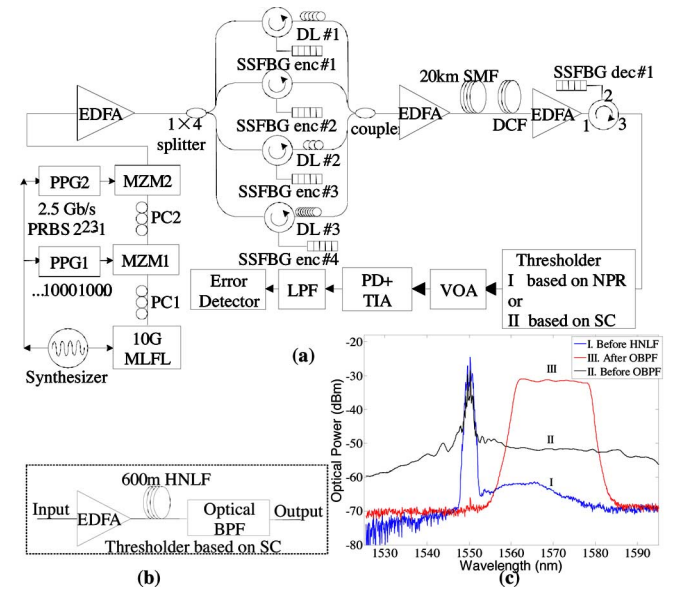


Fig. 3. (a) Experimental setup. (b) Typical threshold based on SC. (c) Measured spectra with the SC-based thresholder: before HNLF (I), before optical BPF (II), and after optical BPF (III). The power levels of the spectra are adjusted for clarity.

then modulated by a Mach-Zehnder intensity modulator with $2^{23} - 1$ pseudorandom binary sequence (PRBS). The amplified optical signal is split into four arms, and then encoded by four different SSFBGs. Optical delay lines with different lengths were used to decorrelate the encoded signals. After this, the encoded signals were recombined, amplified, and launched into a 20-km single-mode fiber (SMF) plus a dispersion compensation module (DCM). At the receiver side, the signal was decoded by an SSFBG decoder and then sent into the NPR-based thresholder. Finally, the signal was detected by a 10-GHz optical receiver followed by a 3.5-GHz low-pass filter (LPF) and sent into an error detector. Note that the FRM used in the thresholder has a bandwidth of ± 15 nm centered at 1550 nm, which makes it possible for colorless operation over C -band. A conventional optical thresholder based on SC was also used for comparison, and its BER performance was compared with that of the proposed NPR-based thresholder. The SC-based thresholder and its measured spectra are shown in Fig. 3(b) and (c), respectively.

The measured eye diagrams are shown in Fig. 4. From Fig. 4(e)–(j), one can see that after thresholding, the “zero”

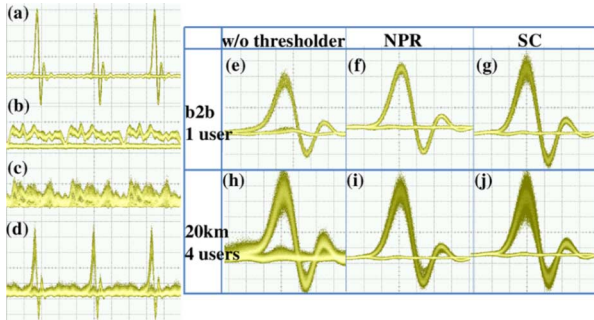


Fig. 4. Measured eye diagrams. (a) Modulated signal; (b) encoded signal, one user; (c) encoded signal, four users; (d) decoded signal after 20-km transmission, four users; (e)–(g) eye diagrams in back-to-back case: (e) before the threshold, (f) after the NPR-based threshold, (g) after the SC-based threshold; and (h)–(j) eye diagrams in 20-km transmission case: (h) before the threshold, (i) after the NPR-based threshold, (j) after the SC-based threshold. The eye diagrams [Fig. 4(g) and (j)] after the SC-based threshold are given for comparison.

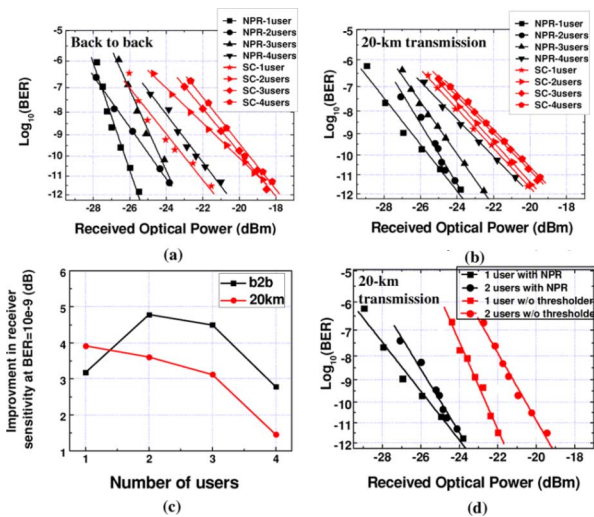


Fig. 5. (a) Measured BER results in a back-to-back case. (b) Measured BER results in a 20-km transmission case. (c) Improvement in the receiver sensitivity for different number of active users, as compared with the case of the SC-based threshold at $\text{BER} = 10E - 9$. (d) BER for 20-km transmission with and without the proposed optical threshold.

bit level is a clear and straight line, indicating that the MAI interference is reduced. However, as the transmission distance or the number of active users increases, the noise on “one” bit level also increases, resulting in a power penalty in the receiver side, which can be seen from Fig. 5. Note that by using the NPR-based threshold, clearer eye diagrams can be obtained [Fig. 4(f) and (i)] as compared with the eye diagrams after SC-based thresholding [Fig. 4(g) and (j)].

The measured BER results for the 2.5-Gb/s OCDMA system using both the NPR- and SC-based thresholders are shown in Fig. 5, with Fig. 5(a) for a back-to-back case and Fig. 5(b) for a 20-km transmission case. In a back-to-back case, the proposed scheme has an improvement in receiver sensitivity of about 2.78 dB over the traditional SC-based threshold, while in the 20-km transmission case, the improvement is about 1.45 dB, as shown in Fig. 5(c). The BER performance after the 20-km

transmission with and without the proposed optical threshold is also shown in Fig. 5(d). Compared with the BER curve with our NPR-based threshold, the power penalty without any optical threshold is 3.43 and 4.45 dB for one user and two users, respectively. When the number of the active users further increases, the BER performance without any optical threshold deteriorates dramatically, and error-free operation cannot be achieved.

IV. CONCLUSION

A novel scheme based on the nonlinear polarization rotation has been proposed in this letter for eliminating the multiple access interference in an ultrashort pulse OCDMA system. The performance of the proposed scheme has been experimentally investigated in our 127-chip SSFBG coding, four-user, 2.5-Gb/s coherent OCDMA system test bed. The proposed scheme has the advantage of colorless operation, which is crucial in, e.g., establishing a large-scale and cost-effective OCDMA passive optical network (PON).

ACKNOWLEDGMENT

The authors would like to thank Dr. Yu and Y. Gao for their experimental helps and fruitful discussions.

REFERENCES

- [1] J. A. Salehi, “Code division multiple-access techniques in optical fiber networks. I. Fundamental principles,” *IEEE Trans. Commun.*, vol. 37, no. 8, pp. 824–833, Aug. 1989.
- [2] L. Xu, I. Glesk, V. Baby, and P. R. Prucnal, “Multiple access interference (MAI) noise reduction in a 2-D optical CDMA system using ultrafast optical thresholding,” in *Proc. IEEE LEOS Annu. Meeting*, 2004, pp. 591–592, Paper WP4..
- [3] P. Petropoulos, N. Wada, P. C. Teh, M. Ibsen, W. Chujo, K. I. Kitayama, and D. J. Richardson, “Demonstration of a 64-chip OCDMA system using superstructured fiber gratings and time-gating detection,” *IEEE Photon. Technol. Lett.*, vol. 13, no. 11, pp. 1239–1241, Nov. 2001.
- [4] Z. Jiang, D. S. Seo, S. D. Yang, D. E. Leaird, R. V. Roussev, C. Langrock, M. M. Fejer, and A. M. Weiner, “Four user 10 Gb/s spectrally phase-coded O-CDMA system operating at 30 fj/bit,” *IEEE Photon. Technol. Lett.*, vol. 17, no. 3, pp. 705–707, Mar. 2005.
- [5] X. Wang, T. Hamanaka, N. Wada, and K. Kitayama, “Dispersion-flattened-fiber based optical threshold for multiple-access-interference suppression in OCDMA system,” *Opt. Exp.*, vol. 13, no. 14, pp. 5499–5505, 2005.
- [6] T. Hamanaka, X. Wang, N. Wada, A. Nishiki, and K. Kitayama, “Ten-user truly asynchronous gigabit OCDMA transmission experiment with a 511-chip SSFBG en/decoder,” *J. Lightw. Technol.*, vol. 24, no. 1, pp. 95–102, Jan. 2006.
- [7] Z. Jiang, D. S. Seo, S. D. Yang, D. E. Leaird, R. V. Roussev, C. Langrock, M. M. Fejer, and A. M. Weiner, “Four-user, 2.5-Gb/s, spectrally coded OCDMA system demonstration using low-power nonlinear processing,” *J. Lightw. Technol.*, vol. 23, no. 1, pp. 143–158, Jan. 2005.
- [8] P. D. Maker and R. W. Terhune, “Study of optical effects due to an induced polarization third order in the electric field strength,” *Phys. Rev.*, vol. 137, no. 3A, pp. A801–A818, 1965.
- [9] V. J. Matsas, T. P. Newson, D. J. Richardson, and D. N. Payne, “Selfstarting passively mode-locked fibre ring soliton laser exploiting nonlinear polarisation rotation,” *Electron. Lett.*, vol. 28, no. 15, pp. 1391–1393, 1992.
- [10] B. Nikolaus, D. Grischkowsky, and A. C. Balant, “Optical pulse reshaping based on the nonlinear birefringence of single-mode optical fibers,” *Opt. Lett.*, vol. 8, no. 3, pp. 189–191, 1983.
- [11] Y. Liu, M. T. Hill, E. Tangdiongga, H. de Waardt, N. Calabretta, G. D. Khoe, and H. J. S. Dorren, “Wavelength conversion using nonlinear polarization rotation in a single semiconductor optical amplifier,” *IEEE Photon. Technol. Lett.*, vol. 15, no. 1, pp. 90–92, Jan. 2003.